Paper based pressure sensor for *green* electronics

Ambarish Paul, Md. Abdul Kafi, Ravinder Dahiya*
Bendable Electronics and Sensing Technologies (BEST) Group, University of Glasgow, G128QQ, United Kingdom
*E-mail: Ravinder.Dahiya@glasgow.ac.uk

Abstract— **This work reports a resistive paper-based disposable pressure sensor based on porous 3D conductive cellulose micro-fiber network. The conductivity in micro-fibers was achieved by subjecting the network to graphene oxide (GO) - poly(3,4-ethylenedioxythiophene) polystyrene sulfonate (PEDOT: PSS) solution. The modified cellulose matrix is sandwiched between graphite paper electrodes so that overall structure is flexible. The device tested in 32-386 Pa range detected a minimum of 34 Pa and exhibited fast dynamic response (in tenths of seconds) with excellent repeatability. The proposed approach for disposable sensors is a step towards green electronics and holds promise for wide range of wearable applications.**

Keywords—cellulose, graphene oxide, pressure sensor

I. INTRODUCTION

Sensitive electronic systems consisting of renewable and biodegradable materials are desirable in many applications such as disposable systems for health monitoring and consumer electronics [1]. The field is also rapidly gaining attention because of current technology leads to electronic-waste which is difficult to recycle and reuse. To combat this problem researchers have reoriented their investigations towards paper and printed electronics, which involves printing eco-friendly materials on disposable substrates such as paper and textile[2-6]. The focus on such disposable systems will support the green electronics agenda and solve the major global challenge related to disposal of devices and environmental sustainability. Among various disposable substrates, the paper is naturally advantageous due to its excellent flexibility, cost effectiveness, disposability, lightweight, and biodegradability, For the last five years there has been a rapid rise in the research activity related to paper based biocompatible devices. Although paper based disposable chemical and electrochemical sensors are widely reported, there is little progress on paper based pressure sensors [7-9]. The biocompatible paper based pressure sensors reported so far can detect minimum pressure (in the order of kPa), which is much higher for most of the wearable applications [10]. For example, blood pressure monitoring using pressure sensors require minimum of 10 Pa. The minimum pressure sensor that has been reported so far with paper based pressure sensors is 60 Pa. However, the device in this case was realized with a complex device architecture by folding of printer papers [11].

Towards larger goal for greener electronics, we present here paper based disposable pressure sensor with enhanced performance. The current challenges related to paper based biocompatible pressure sensors have been addressed in this paper through the development of cellulose paper based device. The device utilizes three-dimensional network of porous conductive micro-fibers as the sensor matrix. The cellulose micro-fibers were made conductive by subjecting them to a conductive solution of graphene oxide (GO) modified poly(3,4-ethylenedioxythiophene) polystyrene sulfonate (PEDOT: PSS) [12-14]. The device is composed of two layers of modified cellulose paper sandwiched between a pair of conductive graphene sheet as electrodes. The graphene sheet eelectrodes retain the flexibility of the device for wide range of applications (Figure 1 inset). The device works on the principle of change in resistance due to the decrease in inter- micro-fiber distance when pressure P is applied normally to the plane of the device.

The work is partly supported by The Royal Society through Newton International Fellowship; European Commission through Marie Curie Fellowship (BEND,H2020-MSCA-IF-2015, 704807) and Engineering and Physical Sciences Research Councils through Fellowship for Growth (PRINTSKIN (EP/M002527/1)

II. EXPERIMENTS

A. *Materials and equipments*

The mono-layered GO and graphite paper was purchased from Graphene Supermarket, NY, USA. The PEDOT:PSS conductive polymer was obtained from Ossila Limited, UK with as received concentration of 1%. The cellulose paper was purchased from Fisher Scientific, (Kimberley Clark™ Tissue paper) UK. The electron microscopic investigation was performed with Hitachi SEM S4700 and the electrical characterization was carried out with Agilent 34461A-6 ½ Digital Multimeter.

B. *Synthesis of GO-PEDOT:PSS composite and device assembly*

The as received PEDOT:PSS (CLEVIOS™ PH 1000) solution was diluted in the ratio of 1:2 with deionised water and 60 µl of the resultant solution was added to 800 µl of four times diluted solution of as received aqueous dispersion of monolayered GO and subsequently mixed using the vortex mixture for 15 min. The cellulose paper was cut into pieces of 1 cm x 0.5 cm dimension and placed on the graphite paper electrode. The cellulose fibers were modified by GO PEDOT:PSS by adding 10 µl of GO-PEDOT:PSS solution to the cellulose fibers and subsequently partially dried in air at room temperature. Two layers of GO-PEDOT:PSS modified cellulose papers were assembled on top of each other and

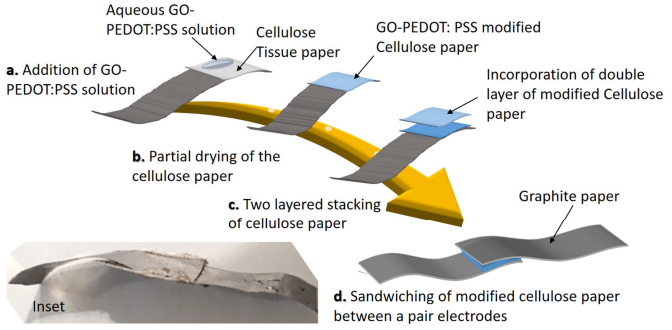

Figure 1: Schematic representation of device process flow (Inset) Optical image of the device

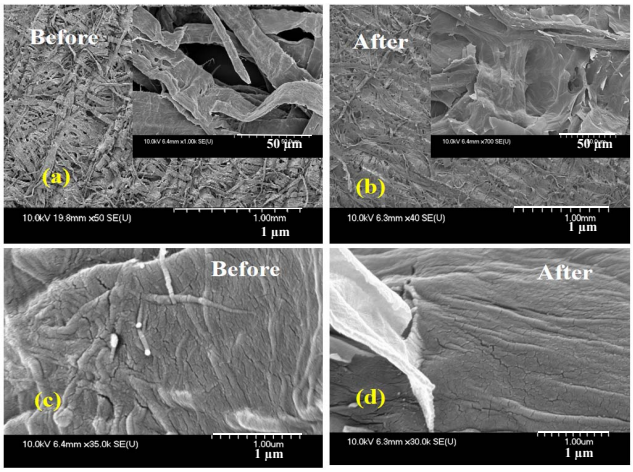

Figure 2: Surface morphology of cellulose paper (a) before and (b) after modification with GO-PEDOT:PSS. Inset: The cellulose micro-fibers (a) before and (b) after modification showing the microfibers covered with GO sheets. (c) Unmodified and (d) GO-PEDOT modified surface of cellulose micro-fibers

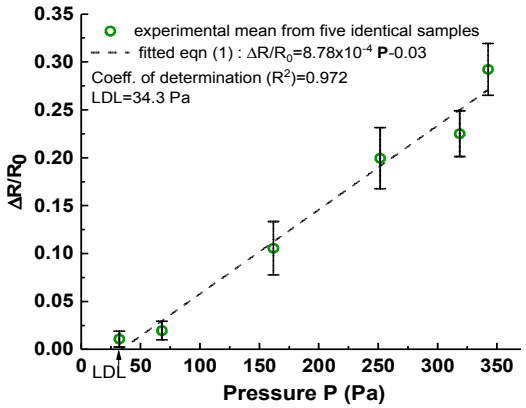

Figure 3: $\Delta R/R_0$ vs. P calibration curve of the device showing LDL=34.3 Pa

sandwiched between a pair of graphite sheet electrode electrodes to form the device. The schematic representation of the device process flow is depicted in Figure 1. Identically prepared GO-PEDOT:PSS modified cellulose paper was characterized under SEM for microstructural investigation of the modified surface.

C. *SEM Investigations*

The SEM investigations were performed before and after GO-PEDOT:PSS modification and the images are shown in Figure 2 (a) and (b) respectively. The SEM images of bare cellulose before treatment revealed that the cellulose fibers are arranged randomly to form uniform and continuous three-dimensional network with pore sizes ranging between 20-30 µm. The surface of the cellulose fibers provides a characteristic rough morphology with striations as shown in Figure 2(c). There is a significant change in the surface morphology of cellulose fibers on treatment with GO-PEDOT:PSS solution as shown in Figure 2 (b). The PEDOT:PSS solution was absorbed by the cellulose fibers which enhances its bulk electrical properties, while the monolayer GO sheets were adhered on the surface, enhancing the surface conductivity of the fibers. Figure 2 (b. inset) shows adhering of GO sheets to the surface of cellulose fibers. Upon externally applied normal pressure, the GO sheets

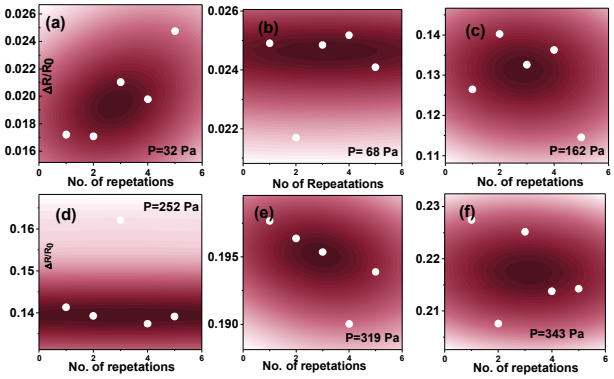

Figure *4*: Probability density representation of the distribution of data points of ΔR/R0 for different repetitive measurements for data sets of P= (a) 32 Pa (b) 68 Pa, (c) 162 Pa, (d)252 Pa, (e) 319 Pa and (f) 343 Pa

facilitates in the transfer of electronic charge to the adjacent one through electron tunnelling. The fiber surface modified with monolayer GO graphene can be distinguished from the untreated fiber through passivation of GO sheets led striations, as shown in Figure 2(c,d). The GO modified cellulose fiber surface due to its high electrical conductivity readily transforms the stimulus into measurable change in electrical resistance.

III. SENSOR PERFORMANCE

The device was characterized with static and dynamic loads with applied pressure equivalent to (a) 32 Pa, (b) 68 Pa, (c) 162 Pa, (d) 252 Pa, (e) 319 Pa and (f) 343 Pa measured over the total sensing area of 1 cm × 0.5 cm as detailed below.

A. *Static loadings*

The electrical measurements were performed with static loads and responses were expressed as variations in resistance with applied normal pressure. The electrical response of the developed pressure sensor under applied normal P was measured using multimeter and the data was acquired remotely using Labview program. The response of the device towards different applied P was investigated through the determination of the ratio $(R_0\text{-}R_f)/R_0=\Delta R/R_0$, where R_0 is the initial resistance before subjection to applied P and R_f is the final resistance on application of static P. The change in resistance ΔR was calculated and normalized with R_0. To neglect effects of baseline shifts on sensor performance the response of the device was captured by studying the ratio $\Delta R/R_0$ for different static P loadings. The experiments were performed on five identical devices to study the reproducibility of fabrication process of the device. The respective data sets from different devices corresponding to different values of P were investigated by determining the respective standard deviations (SD) and mean value. To obtain the calibration curve of the device, the mean values of the respective data sets were fitted in standard linear equation expressed as

$$\Delta R/R0 = \alpha . P - \beta \quad (1)$$

where α represents the slope of the calibration curve and β denotes the intercept on the y-axis. The plot of $\Delta R/R_0$ vs. P calibration curve shows a linear trend with sensitivity $\alpha = 8.78\times10^{-4}$ /Pa in the pressure range of 32-343 Pa as shown in Figure 3. The errors in measurements from different devices were graphically represented as error bars for different data sets. The lower dynamic limit (LDL) of the device was determined by equating the ratio $\Delta R/R_0 = 0$ signifying no sensor response

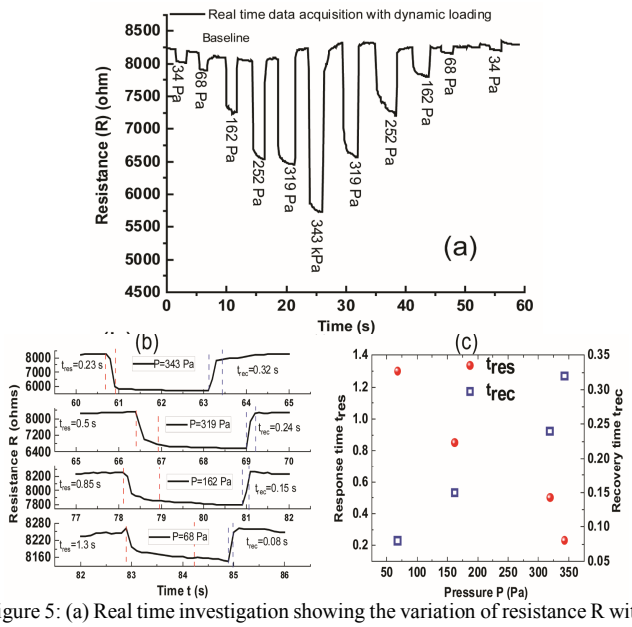

Figure 5: (a) Real time investigation showing the variation of resistance R with different applied P (b) The variation of R with time showing the t_{res} and t_{rec} at different P. (c) Plot of t_{res}/t_{rec} vs. P

under static P. From (1), the LDL was calculated using the relation $P_{LDL} = \beta/\alpha$ to be 34.4 Pa. The repeatability investigations were performed by subjecting the device to five repetitive static measurements, the response of which are depicted in Figure 4 for different static P. The repeatability error was calculated using the relation: $\delta_R = SD/R_{mean}$ (2), where R_{mean} denotes the mean value of respective data set. The δ_R was found to be 10.2% for P = 32 Pa but decreased to 3.5% for P = 343 Pa. The high repeatability error at low P was attributed to (a) the slow response to static P and (b) inconsistencies in the relaxation of the cellulose microfiber matrix after repeated compressions

B. Dynamic loading

The device was characterized under different dynamic loadings in the dynamic range range P=34-382 Pa. The real time investigation of the device under different values of P was performed by measuring the change in resistance of the device under different dynamic loadings as shown in Figure 5(a). The data was recorded for different applied P in forward and reverse P loading-cycles with alternative loading and rest times of 2 s each. The device suffered a baseline shift in the forward P loading-cycle but absent in the reverse P loading cycle. The shift in baseline in the forward P loading cycle was attributed to the lack of enough inertial force generated in the micro-fibers to restore to their initial state when the applied P was withdrawn. However, the cellulose micro-fibers can restore to its initial state due to the increased inertial force in the reverse P loading-cycle. The dynamic response was investigated by determining the response t_{res} and recovery times t_{rec} of the device at different applied P=343, 319, 162 and 34 Pa as shown in Figure 5 (b). The t_{res} of the device decreased from 1.3 s at P=34 Pa to 0.23 s at P=343 Pa while the t_{rec} increased from 0.08 s at 34 Pa to 0.32 s at P=343 Pa. This linear variation of t_{res} and t_{rec} with applied P is shown in Figure 5 (c).

IV. CONCLUSION

The disposable paper based pressure sensors presented here provides enhanced conductive pathways for the electrons to travel between the graphene paper electrode. The conductive pathways based on three-dimensional network of cellulose micro-fibers show reduced electrical resistance under applied pressure. The device involves easy fabrication process and was prepared from biocompatible materials such as PEDOT:PSS and GO. The device shows low lower detection limit (LDL) of 34 Pa and offers a sensitivity of 8.78×10^{-4}/Pa. The device shows excellent dynamic characteristics with fast response and recovery times. More work is needed to address inconsistent response, especially in the lower side of applied pressure range. This could be addressed by increasing the thickness of the cellulose matrix and thinning of the graphite paper electrodes and will be presented in our extended work in the future. The paper based sensors finds application in numerous applications including the pressure assessment of static grip of robotic hand, determination of bandage pressure and other wearable applications such as blood pressure monitoring.

REFERENCES

[1] J. C. Middleton and A. J. Tipton, "Synthetic biodegradable polymers as orthopedic devices," *Biomaterials,* vol. 21, pp. 2335-2346, 2000.

[2] M. Irimia-Vladu, "Green electronics: biodegradable and biocompatible materials and devices for sustainable future," *Chem. Soc. Rev,* vol. 43, pp. 588-610, 2014.

[3] A. Paul and B. Bhattacharya, "DNA Functionalized Carbon Nanotubes for Nonbiological Applications," *Mat. and Manufac. Processes,* vol. 25, pp. 891-908, 2010.

[4] D. Tobjörk and R. Österbacka, "Paper Electronics," *Advanced Materials,* vol. 23, pp. 1935-1961, 2011.

[5] S. Khan, S. Tinku, L. Lorenzelli, and R. S. Dahiya, "Flexible Tactile Sensors Using Screen-Printed P(VDF-TrFE) and MWCNT/PDMS Composites," *IEEE Sensors Journal,* vol. 15, pp. 3146-3155, 2015.

[6] A. Paul, B. Pramanick, B. Bhattacharya, and T. K. Bhattacharyya, "Deoxyribonucleic Acid Functionalized Carbon Nanotube Network as Humidity Sensors," *IEEE Sensors Journal,* vol. 13, pp. 1806-1816, 2013.

[7] P. S. Khiabani, A. H. Soeriyadi, P. J. Reece, and J. J. Gooding, "Paper-Based Sensor for Monitoring Sun Exposure," *ACS Sensors,* vol. 1, pp. 775-780, 2016.

[8] A. M. Lopez-Marzo and A. Merkoci, "Paper-based sensors and assays: a success of the engineering design and the convergence of knowledge areas," *Lab on a Chip,* vol. 16, pp. 3150-3176, 2016.

[9] J. C. Cunningham, P. R. DeGregory, and R. M. Crooks, "New Functionalities for Paper-Based Sensors Lead to Simplified User Operation, Lower Limits of Detection, and New Applications," *Annu. Rev. Anal. Chem,* vol. 9, pp. 1-20, 2016.

[10] K. Lee, J. Lee, G. Kim, Y. Kim, S. Kang, S. Cho, *et al.*, "Rough-Surface-Enabled Capacitive Pressure Sensors with 3D Touch Capability," *Small,* p. 1700368, 2017.

[11] P.-K. Yang, Z.-H. Lin, K. C. Pradel, L. Lin, X. Li, X. Wen, *et al.*, "Paper-Based Origami Triboelectric Nanogenerators and Self-Powered Pressure Sensors," *ACS Nano,* vol. 9, pp. 901-907, 2015.

[12] M. Yang, Y. Zhang, H. Zhang, and Z. Li, "Characterization of PEDOT:PSS as a Biocompatible Conductive Material," *IEEE Int. Conf. on Nano/Micro Engg. and Molecular Sys.* , pp. 149-151, 2015.

[13] W. Dang, V. Vinciguerra, L. Lorenzelli, and R. Dahiya, "Metal-organic Dual Layer Structure for Stretchable Interconnects," *Procedia Eng,* vol. 168, pp. 1559-1562, 2016.

[14] W. Dang, L. Lorenzelli, V. Vinciguerra, and R. Dahiya, "Hybrid Structure of Stretchable Interconnect for Reliable E-skin Application," *Industrial Electronics (ISIE)-IEEE,* pp. 2093-2096, 2017.